Unpinning of spiral waves by electrical forcing in excitable chemical media

Malee Sutthiopad,[1] Jiraporn Luengviriya,[2,3] Porramain Porjai,[1] Boosayarat Tomapatanaget,[4]
Stefan C. Müller,[5] and Chaiya Luengviriya[1,*]

[1]*Department of Physics, Kasetsart University, 50 Phaholyothin Road, Jatujak, Bangkok 10900, Thailand*
[2]*Department of Industrial Physics and Medical Instrumentation, King Mongkut's University of Technology North Bangkok, 1518 Pibulsongkram Road, Bangkok 10800, Thailand*
[3]*Lasers and Optics Research Group, King Mongkut's University of Technology North Bangkok, 1518 Pibulsongkram Road, Bangkok 10800, Thailand*
[4]*Department of Chemistry, Chulalongkorn University, Bangkok 10330, Thailand*
[5]*Institute of Experimental Physics, Otto-von-Guericke University Magdeburg, Universitätsplatz 2, D-39106 Magdeburg, Germany*
(Received 12 February 2014; published 8 May 2014)

We present experimental observations on the electrically forced release of spiral waves pinned to unexcitable circular obstacles in the Belosov-Zhabotinsky reaction. When the applied electric current density reaches the necessary current density J_{unpin}, the spiral tip is detached and subsequently drifts away from the obstacle. J_{unpin} is found to increase with the obstacle diameter d. The growth rate $\Delta J_{\mathrm{unpin}}/\Delta d$ is much higher for obstacles larger than the free spiral core compared to that for smaller obstacles. The experimental findings are confirmed by numerical simulations using the Oregonator model. The results imply that it is more difficult to release spiral waves pinned to larger obstacles, especially when the obstacle size exceeds that of the free spiral core.

DOI: 10.1103/PhysRevE.89.052902 PACS number(s): 05.45.−a, 05.65.+b, 82.40.Ck, 82.40.Qt

I. INTRODUCTION

Spiral waves evolve in different excitable media, e.g., during CO oxidation on a platinum surface [1], cell aggregation in slime mold colonies [2], electrical wave propagation in cardiac tissues [3], and concentration waves in the Belousov-Zhabotinsky (BZ) reaction [4,5]. Such spiral patterns of electrical excitation in the heart and their instabilities are involved in causing certain types of cardiac arrhythmia, such as ventricular tachycardia and fibrillations [6,7], which can potentially lead to sudden cardiac death.

Annihilation of spiral waves is possible when the waves drift until they hit the boundary of the medium. Even though this drift and annihilation can occur naturally, spiral waves in cardiac tissues are often stabilized by being pinned to local heterogeneities (e.g., veins or scars), which act as obstacles [3]. Note that obstacles may either attract or repulse spiral waves depending on the distance between the spiral core centers and the obstacles [8,9]. Furthermore, it has been predicted [10,11] that obstacles cause the period of pinned spiral waves to increase with the obstacle size. A systematic study of pinned spiral waves in a thin layer of the photosensitive ruthenium-catalyzed BZ reaction [12] has revealed that wave period, wavelength, and velocity increase with the size of a circular unexcitable obstacle created by a laser spot. For three-dimensional BZ media, spiral structures known as scroll rings are often observed to contract and eventually self-annihilate [13,14]. The intrinsic contraction is suppressed, when a scroll ring is pinned to an obstacle [15,16].

It has been demonstrated that low-energy shocks, produced by virtual electrode polarization [17], can unpin and terminate ventricular tachycardia in isolated rabbit ventricles [18] and cell cultures of neonatal rat ventricular myocytes [19,20]. Other low-energy methods use a high-frequency train of electrical stimuli to eliminate spiral waves in cardiac tissue cultures by inducing unpinning and drift of the waves, until they collide with the boundary of the medium [21,22]. Such an external wave train is used to release a spiral wave pinned to a cluster of small droplets of oil in the BZ reaction [23].

In this article, we present an investigation of the electrically forced unpinning of spiral waves in BZ media. In the absence of obstacles, an applied electrical current results in an advective motion of ionic species and induces a drift of the spiral tips along a straight path. The drift velocity is found to increase with the magnitude of applied current [24–26]. Our experiments are performed in uniform thin layers of the BZ reaction [27] using chemically inert plastic cylinders with well-defined diameters as unexcitable obstacles. Thus, the relation between the strength of forcing and the obstacle size is precisely specified. We perform simulations using the Oregonator model [28,29] in close correspondence with the experimental results.

II. EXPERIMENTS

A. Methods

The Belousov-Zhabotinsky (BZ) solutions are prepared from $NaBrO_3$, H_2SO_4, malonic acid (MA) and ferroin, all purchased from Merck. Stock solutions of $NaBrO_3$ (1 M) and MA (1 M) are freshly produced by dissolving powder in deionized water (conductivity of $\sim$0.056 μS cm^{-1}), whereas stock solutions of H_2SO_4 (2.5 M) and ferroin (25 mM) are commercially available. To prevent any hydrodynamic perturbation, the reaction is embedded in a 1.0% wt/wt agarose gel (Sigma). Appropriate volumes of the stock solutions are mixed and diluted in deionized water to form BZ solutions with initial concentrations: $[H_2SO_4]$ = 200 mM, [MA] = 50 mM, $[NaBrO_3]$ = 50 mM, and [ferroin] = 0.625 mM. The temperature is controlled at 24 °C ± 1 °C. In the absence of electrical forcing as well as any obstacle, these BZ media

*Corresponding author: fscicyl@ku.ac.th

support rotating spiral waves, the tip of which (measured location as in Ref. [27]) moves around a circular area (i.e., the spiral core) with a diameter of 0.75 mm. The wave period is about 4 min.

Unpinning of spiral waves by electrical forcing is studied in a uniform thin layer of the BZ reaction using a flat reactor constructed from transparent Plexiglas [27]. The volume is $100 \times 100 \times 1.0$ mm^3. An electric field is applied via two electrodes in electrolytic compartments (size of each $25 \times 100 \times 2.0$ mm^3), which are attached to the left and the right boundaries of the main volume [14]. Application of the electric field also results in gas bubbles formed by electrolysis. The bubbles cause the resistance between the electrodes to fluctuate in time. To specify precisely the strength of forcing, electricity driven by a power supply in a constant electrical current mode is utilized, and the strength of applied electrical forcing in the experiments is recorded as electrical current density instead of electric field, which is normally used in simulations. As an obstacle, a chemically inert plastic cylinder with a diameter of 0.4–1.5 mm and a height of 1.0 mm is attached in the main volume by using silicone paste before the BZ solution is filled into the reactor. During the experiments, the reactor is placed in a transparent thermostating bath to remove Ohmic heat and to set the temperature at 24 °C ± 1 °C. The bath is put between a white light source and a color CCD camera (Super-HAD, Sony) to record the images of the medium every second with a resolution of 0.05 mm pixel^{-1}.

A spiral wave pinned to the obstacle is initiated by the following procedure: The reactor is oriented vertically, and a volume of BZ solution is filled into the reactor, forming the first layer of 2.5 cm height, where the obstacle is located. Then, we wait until the gel is formed. Wave fronts are initiated by immersion of a silver wire of 0.5 mm diameter between the left edge of the reactor and the obstacle. One open end of the wave front propagates towards the obstacle [Fig. 1(a)], while the other moves close to the left edge of the reactor. Another volume of the BZ solution is added to the reactor as the second layer when the open end reaches the obstacle [Fig. 1(b)]. The final height of the medium is about 4.5–5.0 cm. Shortly after filling in the second layer, the open end of the wave front starts to curl in [Fig. 1(c)] to form a spiral wave with its tip rotating around the obstacle [Fig. 1(d)].

B. Results and discussion

Figure 1 shows the development of a pinned spiral wave in our experiments. As reported earlier [27,30,31], the atmospheric oxygen suppresses the excitability of a thin sheet below the top surface of the first layer [dark orange (dark gray) band in Figs. 1(a)–1(c)], so that the wave front does not reach the atmospheric interface. After the second layer is filled, this inhibited layer disappears when the dissolved oxygen is consumed during the first passage of the excitation front [see Fig. 1(c)]. We note that filling in the BZ solution to form the second layer must be done at the proper time, i.e., when the front reaches the obstacle, as depicted in Fig. 1(b). If this is done too early or too late (i.e., when the front does not touch the obstacle), the spiral wave will not be pinned.

For obstacles larger than the free spiral core, the tips of pinned spiral waves are always attached to the obstacle [as in Fig. 1(d)]. In contrast, we observe alternations of attachment [Figs. 2(a) and 2(b)] and detachment [Figs. 2(c) and 2(d)] of the spiral tip in the vicinity of obstacles smaller than the free spiral core. The spiral core is an area in the refractory state, thus no wave can propagate into it. When a small obstacle occupies some part of the spiral core, the other (unoccupied) part is still in the refractory state and prohibits any wave propagation. As in Figs. 2(c) and 2(d), the spiral tip is temporarily detached from the obstacle, when it reaches such a refractory area. However, the free tip moves towards the obstacle again.

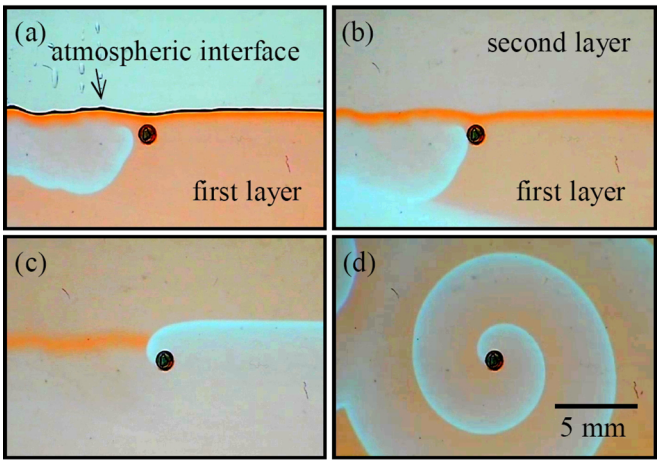

FIG. 1. (Color online) Pinning a spiral wave in the BZ reaction. (a) A wave front is initiated by a silver wire in the first layer. (b) A portion of the BZ reaction is placed on top as the second layer, when the blue (light gray) front end reaches the obstacle (black circle; diameter of 1.05 mm). (c) The inhibited layer [dark orange (dark gray) band] disappears after the first passage of the wave front. (d) After three spiral rotations, the front adopts a typical spiral structure with its tip attached to the obstacle.

To investigate unpinning phenomena, we apply a constant current density J, which is stepwise increased from small to large values. For each value of the obstacle diameter, the

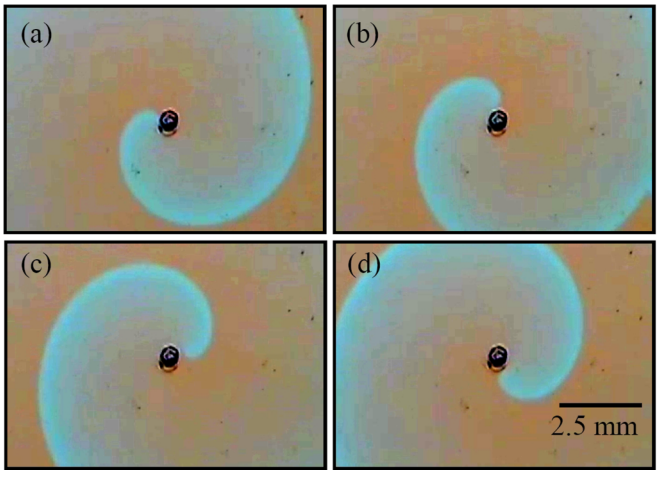

FIG. 2. (Color online) Motion of a spiral wave around a small obstacle in the BZ reaction. For each rotation, the spiral tip is alternately (a) and (b) attached to and (c) and (d) detached from the obstacle with a diameter of 0.4 mm.

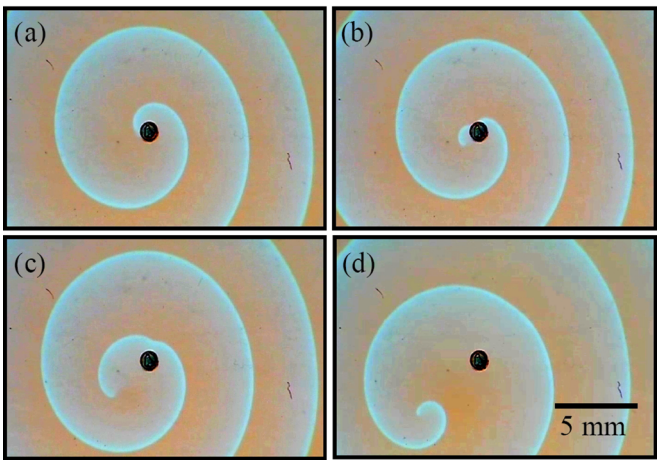

FIG. 3. (Color online) Unpinning of a spiral wave by electrical forcing in the BZ reaction. The obstacle diameter is 1.05 mm. The positive and negative electrodes are placed on the left- and the right-hand sides, respectively. (a) An electrical current density $J = 96$ mA cm^{-2} induces an anisotropic spiral structure with its tip still attached to the obstacle. When J reaches a critical value $J_{\text{unpin}} = 98$ mA cm^{-2}, (b) the spiral tip is detached and (c) and (d) subsequently moves away from the obstacle.

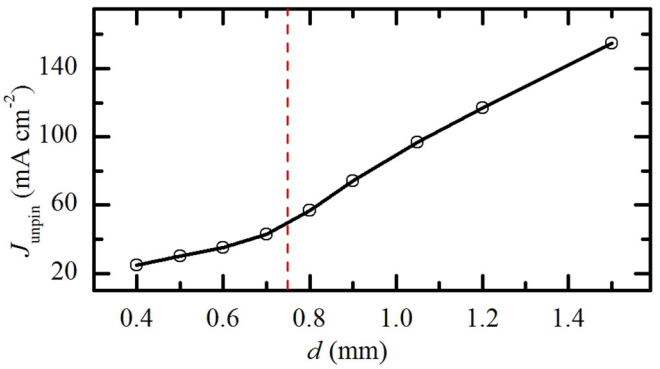

FIG. 4. (Color online) Electrical current density J_{unpin} necessary for releasing a spiral wave pinned to an unexcitable obstacle with diameter d. The vertical dashed line at 0.75 mm indicates the core diameter of a free spiral wave.

experiments are performed twice with different steps $\Delta J = 10$ and 2 mA cm^{-2}, respectively. In all experiments, each value of J is applied for an interval of three to five spiral rotations before J is increased. The spiral tip leaves the obstacle and moves away when J reaches a critical value J_{unpin}, i.e., the minimal current density for unpinning. For guidance, the first experiment with the large step $\Delta J = 10$ mA cm^{-2} provides a rough estimate of electrical current density necessary for unpinning the spiral wave. The fine-tuning of J is obtained in the second experiment with $\Delta J = 2$ mA cm^{-2}. This way, one can obtain the finest value of J_{unpin} ($\Delta J = 2$ mA cm^{-2}) available from our equipment within a relatively short observation time of up to 2 h, while the aging of the BZ reaction, which potentially affects the dynamics of the spiral wave in long running experiments, can be minimized.

Figure 3 demonstrates the unpinning phenomenon. With $J < J_{\text{unpin}}$, the spiral tip still remains attached to the obstacle. However, the forcing induces an anisotropically distorted spiral wave [see Fig. 3(a)] because the electrical current accelerates or decelerates the front propagating towards or away from the positive electrode [26], while the spiral tip remains pinned. For $J \geq J_{\text{unpin}}$, the spiral tip is detached from the obstacle [see Fig. 3(b)]. When the electrical current is continuously applied, the unpinned spiral tip moves towards the positive electrode with an angle. The anisotropic structure also changes with time [see Figs. 3(b)–3(d)]. As the spiral tip moves far away from the obstacle [Fig. 3(d)], we observed the deformed wave structure similar to a drifting spiral wave under electrical forcing in the absence of obstacles [24].

The necessary current density J_{unpin} for unpinning the spiral wave increases with the obstacle diameter d, as shown in Fig. 4. For obstacles smaller than the free spiral core ($d < 0.75$ mm), J_{unpin} increases with d, but the increase is slower than that for larger obstacles ($d > 0.75$ mm). To investigate the growth rate $\Delta J_{\text{unpin}}/\Delta d$, we apply linear fits for the two ranges of the obstacle diameter and find that $\Delta J_{\text{unpin}}/\Delta d = 0.590 \pm 0.052$ and 1.389 ± 0.048 A cm^{-3} for $d < 0.75$ mm and $d > 0.75$ mm, respectively. Clearly, J_{unpin} grows at a much higher rate for the large obstacles in comparison with that for the small ones. The results show that it is more difficult to release spiral waves pinned to larger obstacles, especially when the obstacle size exceeds that of the free spiral core.

III. SIMULATIONS

A. Methods

In our numerical simulations, we use the two-variable Oregonator model to describe the dynamics of the activator u and the inhibitor v (corresponding to the concentrations of $HBrO_2$ and the catalyst, respectively) in the BZ reaction. The advection terms for both u and v account for the electric field E applied in the x direction:

$$\frac{\partial u}{\partial t} = \frac{1}{\varepsilon}\left(u - u^2 - f v \frac{u-q}{u+q}\right) + D_u \nabla^2 u - M_u E \frac{\partial u}{\partial x},$$
$$\frac{\partial v}{\partial t} = u - v + D_v \nabla^2 v - M_v E \frac{\partial v}{\partial x}. \quad (1)$$

As in Refs. [14,29], the parameters are chosen as $\varepsilon = 0.01$, $q = 0.002$, $f = 1.4$, the diffusion coefficients $D_u = 1.0$ and $D_v = 0.6$, and the ionic mobilities $M_u = -1.0$ and $M_v = 2.0$. In the absence of an electric field, the tip of a free spiral wave rotates around a circular core [diameter = 0.9 system unit (s.u.)]. The spiral tip is defined as the intersection of the contour $u = 0.15$ and $v = 0.0935$ to ensure $\partial u/\partial t = 0$ on the position of the tip [14].

The simulations are performed using an explicit Euler method with a nine-point approximation of the two-dimensional Laplacian operator and a centered-space approximation of the gradient term. The uniform grid space $\Delta x = \Delta y = 0.025$ s.u. and the time step $\Delta t = 1.9 \times 10^{-4}$ time unit (t.u.) are chosen as required for numerical stability [$\Delta t \leq (3/8)(\Delta x)^2$ [32]]. The dimensionless size of the system is 20 × 20 s.u. (corresponding to 800 × 800 grid points). A completely unexcitable circular area is put as the obstacle. Therefore, the boundaries of both the medium and the obstacle have no-flux conditions.

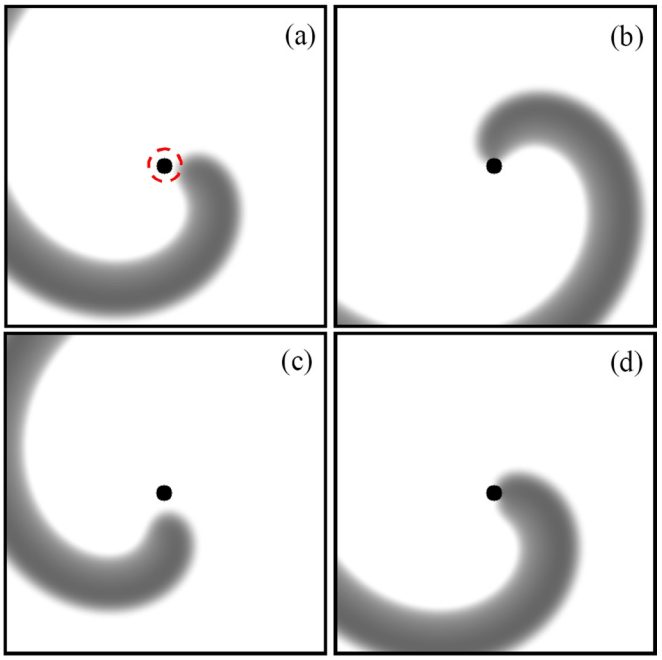

FIG. 5. (Color online) Motion of a spiral wave around a small obstacle in the Oregonator model. (a) At the beginning, an obstacle 0.5 s.u. in diameter is put in the middle of the spiral core (the dashed circle). (b) The tip moves towards and is attached to the obstacle. (c) Subsequently, it is detached from the obstacle, but (d) it is attached to the obstacle again.

To create a spiral wave, a planar wave is triggered by setting a five-grid-point strip at an edge of the medium to an excited state (e.g., $u = 1.0$ and $v = 0$ for $0.0 \le x \le 0.5$). The wave front is allowed to propagate into the middle of the medium before half of the medium is reset to an excitable state (e.g., $u = 0$ and $v = 0$ for $0.0 \le y \le 10.0$), leading to a free-end wave front, which subsequently curls to form a rotating spiral wave. The circular obstacle (diameter d of 0.2–1.9 s.u.) is put in the middle of the spiral core after the spiral wave is allowed to propagate freely for several rotations.

B. Results and discussion

The obstacles affect the movement of the spiral tip in the same ways as found in our experiments. In the case of large obstacles, the spiral tip is simply attached to the obstacle at all times. However, alternations of attachment and detachment of the spiral tip to the obstacle smaller than the free spiral core are observed. Figure 5 illustrates the dynamics of the spiral tip in the vicinity of such a small obstacle with $d = 0.5$ s.u. Shortly after the obstacle is put into the spiral core [see Fig. 5(a)], the spiral tip leaves its circular path (the dashed circle) and moves closer to the obstacle until getting attached to it [Fig. 5(b)]. Subsequently, the spiral tip is detached from the obstacle and moves away for a short distance [Fig. 5(c)] before moving back and being attached to the obstacle again [Fig. 5(d)].

As in our experimental results, the pinned spiral wave in the simulations is forced to drift away from the obstacle only when the applied electric field E reaches the critical value E_{unpin} (the electric field necessary for unpinning). Figure 6 demonstrates the dynamics of a pinned spiral wave under the applied field. When $E = 0.625$, which is very close to but weaker than E_{unpin}, the spiral tip is alternately detached from [Figs. 6(a), 6(b), and 6(d)] and attached to [Figs. 6(c) and 6(e)] the obstacle.

The unpinning is successful at a slightly stronger field $E = 0.630$. At the beginning, the motion of the spiral tip seems similar to that at the weaker field [compare Figs. 6(a) and 6(b) with 6(a′) and 6(b′)]. On collision with the obstacle in Figs. 6(b) and 6(b′), a part of the front end (indicated by the arrows) is separated from the spiral wave. For $E = 0.625$, this small segment of the broken front end contracts until it

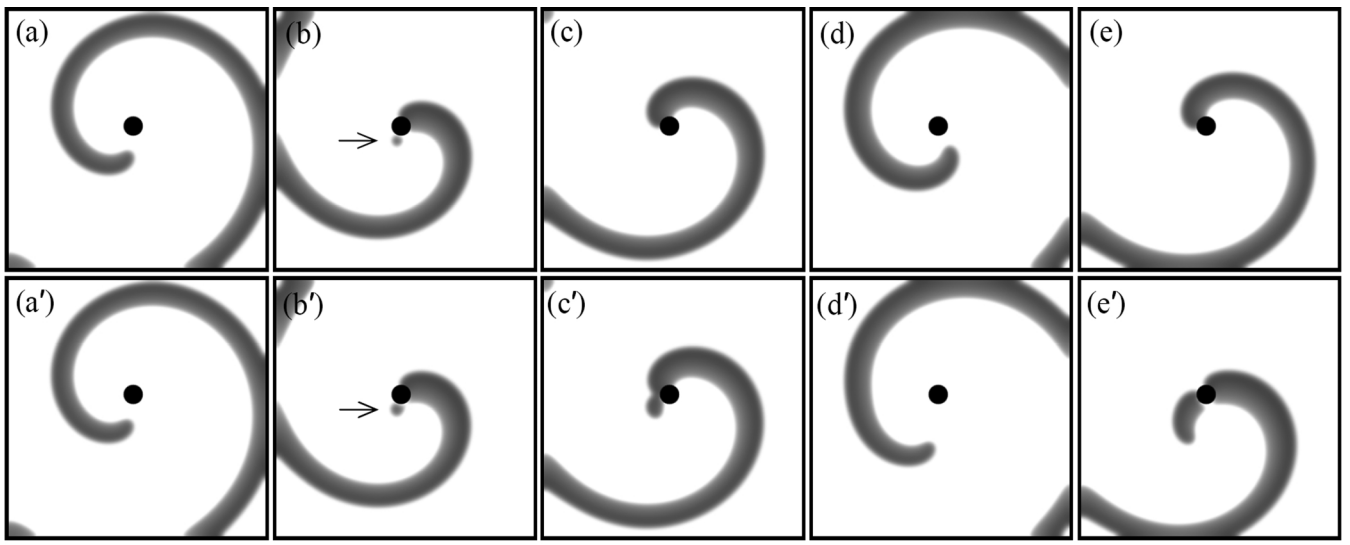

FIG. 6. Effect of an electrical field on a pinned spiral wave in the Oregonator model. The obstacle diameter is 1.5 s.u. The direction of the electric field E is pointing to the right of the images. (a)–(e) Forced temporary detachments: The spiral tip is alternately attached to and detached from the obstacle under $E = 0.625$. (a′)–(e′) Unpinning: The spiral tip is detached and moves away from the obstacle under $E = 0.630$. The arrows indicate the segments of broken front end.

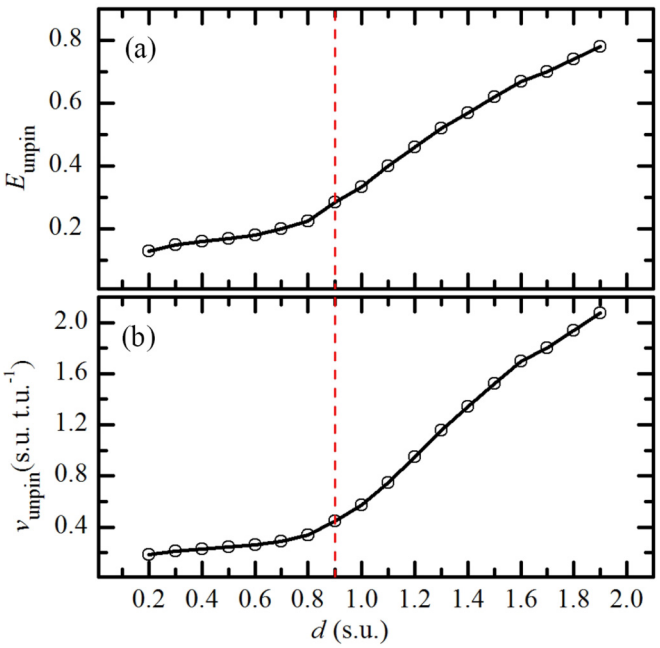

FIG. 7. (Color online) Necessary forcing to release a spiral wave pinned to an unexcitable obstacle with diameter d in the Oregonator model: (a) the electrical field E_{unpin} and (b) the corresponding drift velocity v_{unpin}. The vertical dashed line at 0.9 s.u. indicates the core diameter of a free spiral wave.

disappears, so that the spiral wave is attached to the obstacle again [Fig. 6(c)]. In contrast, this segment grows at $E = 0.630$ and subsequently merges to the spiral structure, so that the spiral tip does not touch the obstacle [Fig. 6(c′)]. The spiral tip drifts farther away from the obstacle over the course of time [see Figs. 6(a′)–6(e′)]; that is, the spiral wave is successfully unpinned from the obstacle.

The simulations not only reproduce the forced unpinning in our experiments but also reveal the forced temporary detachments around large obstacles [e.g., Figs. 6(a)–6(e)], which are not observed in the BZ reaction. We conjecture that the finest step of the electrical current density ($\Delta J = 2$ mA cm^{-2}) might be insufficiently small to allow these phenomena to occur in our experiments.

Figure 7(a) depicts the necessary applied field E_{unpin} to unpin the spiral wave for different obstacle diameters d. Linear fits provide an approximation of the growth rate $\Delta E_{unpin}/\Delta d = 0.145 \pm 0.011$ and 0.501 ± 0.016 s.u.$^{-1}$ for $d <$ 0.9 s.u. and $d > 0.9$ s.u. This increment of E_{unpin} with a much higher rate for obstacles larger than the free spiral core agrees well with the experiments (Fig. 4). To generalize the forcing, we performed additional simulations by applying the electric field E_{unpin} [the same values as in Fig. 7(a)] to a free spiral wave (without obstacle) and measured the corresponding drift velocity (v_{unpin}) of the spiral tip. As shown in Fig. 7(b), the dependence of v_{unpin} on the obstacle size is similar to that of E_{unpin}: the growth rate $\Delta v_{unpin}/\Delta d = 0.227 \pm 0.022$ and 1.69 ± 0.045 s.u.$^{-1}$ for $d < 0.9$ s.u. and $d > 0.9$ s.u.

The systematic studies in both experiments (Fig. 4) and simulations (Fig. 7) show that unpinning of spiral waves occurs under relative small forcing, when the obstacles are smaller than the free spiral core. This may be because the spiral tip is not tightly attached to those small obstacles: Its temporary detachments occur when the tip reaches the refractory area (Figs. 2 and 5) even in the absence of external forcing. In contrast, the spiral tip always touches larger obstacles.

Our investigation shows that stronger electrical forcing is needed for unpinning a spiral wave from a larger unexcitable obstacle in chemical media. This requirement of sufficient electrical forcing is consistent with earlier studies on unpinning by an external wave train [11,23,33], where the unpinning is successful only when the frequency of the wave train is higher than the critical value, which increases with the obstacle size. Since the highest frequency of waves is limited by the refractory time of the excitable medium, such unpinning is impossible when the obstacle is very large [11,23]. For some conditions, the pinned spiral wave can be released by the wave train only when the obstacle is smaller than the free spiral core [33]. It is demonstrated [33–35] that the situations can be improved by reducing the excitability of the medium, which leads to an enlargement of the spiral core size.

IV. CONCLUSIONS

We have presented an investigation of the release of a pinned spiral wave in the BZ reaction by electrical forcing. Under a small electrical current density, the spiral wave still remains pinned to an unexcitable cylindrical obstacle. When the electrical current density reaches a critical threshold, the spiral wave is released. The critical current density increases linearly stepwise with the diameter of the obstacle: it grows at a much higher rate for obstacles larger than the free spiral core in comparison to that of smaller obstacles. The experimental results are confirmed by simulations using the Oregonator model. From both parts of this study, we conclude that a release of a pinned spiral wave by an electric forcing is feasible for obstacle sizes both smaller and larger than the free spiral core. However, the study of such electrically forced unpinning becomes a tough endeavor when the wave is pinned to an obstacle larger than the free spiral core.

ACKNOWLEDGMENTS

We thank the Faculty of Science, the Research and Development Institute (KURDI), the Center for Advanced Studies of Industrial Technology, and the Graduate School, Kasetsart University; the German Academic Exchange Service (DAAD); and the Thailand Research Fund (Grant No. TRG5680044) for financial support.

[1] S. Nettesheim, A. von Oertzen, H. H. Rotermund, and G. Ertl, J. Chem. Phys. **98**, 9977 (1993).
[2] F. Siegert and C. J. Weijer, J. Cell Sci. **93**, 325 (1989).
[3] J. M. Davidenko, A. M. Pertsov, R. Salomonz, W. Baxter, and J. Jalife, Nature (London) **355**, 349 (1992).
[4] A. T. Winfree, Science **175**, 634 (1972).
[5] A. T. Winfree, Science **181**, 937 (1973).
[6] A. T. Winfree, Science **266**, 1003 (1994).
[7] E. M. Cherry and F. H. Fenton, New J. Phys. **10**, 125016 (2008).

[8] A. P. Muñuzuri, V. Pérez-Muñuzuri, and V. Pérez-Villar, Phys. Rev. E **58**, R2689 (1998).
[9] C. W. Zemlin and A. M. Pertsov, Phys. Rev. Lett. **109**, 038303 (2012).
[10] J. P. Keener and J. J. Tyson, Physica D (Amsterdam, Neth.) **21**, 307 (1986).
[11] Y.-Q. Fu, H. Zhang, Z. Cao, B. Zheng, and G. Hu, Phys. Rev. E **72**, 046206 (2005).
[12] O. Steinbock and S. C. Müller, Physica A (Amsterdam, Neth.) **188**, 61 (1992).
[13] K. I. Agladze, R. A. Kocharyan, and V. I. Krinsky, Physica D (Amsterdam, Neth.) **49**, 1 (1991).
[14] C. Luengviriya, S. C. Müller, and M. J. B. Hauser, Phys. Rev. E **77**, 015201 (2008).
[15] Z. Jiménez, B. Marts, and O. Steinbock, Phys. Rev. Lett. **102**, 244101 (2009).
[16] Z. Jiménez and O. Steinbock, Europhys. Lett. **91**, 50002 (2010).
[17] I. R. Efimov, Y. N. Cheng, M. Biermann, D. R. Van Wagoner, T. Mazgalev, and P. J. Tchou, J. Cardiovasc. Electrophysiol. **8**, 1031 (1997).
[18] C. M. Ripplinger, V. I. Krinsky, V. P. Nikolski, and I. R. Efimov, Am. J. Physiol. Heart Circ. Physiol. **291**, 184 (2006).
[19] J. Cysyk and L. Tung, Biophys. J. **94**, 1533 (2008).
[20] M. Hörning, A. Isomura, K. Agladze, and K. Yoshikawa, Phys. Rev. E **79**, 026218 (2009).
[21] K. Agladze, M. W. Kay, V. Krinsky, and N. Sarvazyan, Am. J. Physiol. Heart Circ. Physiol. **293**, 503 (2007).
[22] A. Isomura, M. Hörning, K. Agladze, and K. Yoshikawa, Phys. Rev. E **78**, 066216 (2008).
[23] M. Tanaka, A. Isomura, M. Hörning, H. Kitahata, K. Agladze, and K. Yoshikawa, Chaos **19**, 043114 (2009).
[24] O. Steinbock, J. Schütze, and S. C. Müller, Phys. Rev. Lett. **68**, 248 (1992).
[25] K. I. Agladze and P. De Kepper, J. Phys. Chem. **96**, 5239 (1992).
[26] A. P. Muñuzuri, V. A. Davydov, V. Pérez-Muñuzuri, M. Gómez-Gesteira, and V. Pérez-Villar, Chaos Solitons Fractals **7**, 585 (1996).
[27] C. Luengviriya, U. Storb, M. J. B. Hauser, and S. C. Müller, Phys. Chem. Chem. Phys. **8**, 1425 (2006).
[28] R. J. Field and R. M. Noyes, J. Chem. Phys. **60**, 1877 (1974).
[29] W. Jahnke and A. T. Winfree, Int. J. Bifurcation Chaos Appl. Sci. Eng. **1**, 445 (1991).
[30] A. F. Taylor, B. R. Johnson, and S. K. Scott, J. Chem. Soc. Faraday Trans. **94**, 1029 (1998).
[31] A. F. Taylor, B. R. Johnson, and S. K. Scott, Phys. Chem. Chem. Phys. **1**, 807 (1999).
[32] M. Dowle, R. M. Mantel, and D. Barkley, Int. J. Bifurcation Chaos Appl. Sci. Eng. **7**, 2529 (1997).
[33] A. Pumir, S. Sinha, S. Sridhar, M. Argentina, M. Hörning, S. Filippi, C. Cherubini, S. Luther, and V. Krinsky, Phys. Rev. E **81**, 010901(R) (2010).
[34] Z. Y. Lim, B. Maskara, F. Aguel, R. Emokpae, and L. Tung, Circulation. **114**, 2113 (2006).
[35] C. Cabo, A. M. Pertsov, J. M. Davidenko, W. T. Baxter, R. A. Gray, and J. Jalife, Biophys. J. **70**, 1105 (1996).